JoT JOURNAL OF TURBULENCE

http://jot.iop.org/

Direct numerical simulation of spatially developing, three-dimensional swirling jets*

Michael R Ruith† and Eckart Meiburg

Department of Mechanical and Environmental Engineering, University of California, Santa Barbara, CA 93106, USA
E-mail: ruith@engineering.ucsb.edu

Received 9 October 2002
Published 30 December 2002

Abstract. Vortex breakdown of nominally axisymmetric, swirling incompressible jets and wakes issuing into a semi-infinite domain is studied by means of direct numerical simulations, as well as local and global linear stability analyses. A two-parametric low entrainment velocity profile for which the steady, axisymmetric breakdown is well studied (Grabowski W J and Berger S A 1976 *J. Fluid Mech.* **75** 525–44) is selected to discuss the role of the applied swirl in the existence and mode selection of vortex breakdown. As the swirl parameter is increased, bubble, helical and double-helical breakdown modes are observed for the moderate Reynolds number applied. It is shown that a local transition from super- to subcritical flow, as defined by Benjamin (Benjamin T B 1962 *J. Fluid Mech.* **14** 593–629), accurately predicts the swirl parameter yielding breakdown. Thus the basic form of breakdown is axisymmetric. A transition to helical breakdown modes is shown to be caused by a sufficiently large pocket of absolute instability in the wake of the bubble, giving rise to a self-excited global mode. Preliminary axisymmetric results of a global linear instability analysis agree favourably with the direct numerical simulation and thus encourage extension of the global analysis to helical modes.

PACS numbers: 02.70.Ns, 47.27.Wg, 47.20.Ft

* This article was chosen from Selected Proceedings of the 4th International Workshop on Vortex Flows and Related Numerical Methods (UC Santa-Barbara, 17–20 March 2002) ed E Meiburg, G H Cottet, A Ghoniem and P Koumoutsakos.

† Author to whom any correspondence should be addressed.

 PII: S1468-5248(02)54720-2 1468-5248/02/000001+8$30.00

Contents

1. Introduction

Vortex breakdown of swirling flows is characterized by an abrupt structural change of the nominally axisymmetric core of a swirling jet, forming an internal stagnation point. Experimental evidence manifests the existence of three distinct breakdown modes: bubble, helical and double helical. Despite extensive theoretical, experimental and numerical research for over 40 years, a general explanation for the existence and mode selection of vortex breakdown is still elusive.

To shed light on the mechanism determining the existence and mode selection of vortex breakdown in incompressible, laminar flow in an unconfined domain, a numerical investigation [4] is undertaken. The obtained axisymmetric and three-dimensional results are discussed in light of classical wave theory, recent local absolute/convective instability results and global linear instability results.

2. Discussion of results

We shall limit ourselves to a low entrainment velocity profile [1] which is assumed at each axial position at time $t = 0$ and is kept constant at the inflow boundary as the flow evolves. However we wish to point out that, for the moderate Reynolds number considered, a similar dynamical evolution is obtained for pronounced top-hat profiles modelling recent water tank experiments [3]. The velocity components v_r, v_θ, v_z in radial, azimuthal and axial directions are defined by the parameter combination S and α. The swirl parameter S represents the ratio of azimuthal velocity at the core edge $r = R$ and axial velocity at infinity, i.e. $S = v_\theta(R)/v_{z,\infty}$. The coflow parameter α represents the ratio of the axial velocity at the axis to the axial velocity in the free stream, i.e. $\alpha = v_{z,c}/v_{z,\infty}$. Setting α greater or less than one yields jet or wakelike profiles, respectively. The profile is nondimensionalized by the characteristic core radius R and the free stream axial velocity $v_{z,\infty}$. The properties of the Grabowski profile are sketched in figure 1.

To simulate a spatially and temporally evolving jet, the outflow and lateral boundaries employ radiation conditions. Allowing for mass and momentum flux through the radial boundary permits the selection of relatively small radial domain sizes without artificially confining the flow. Despite the additional mass exchange over the radial boundary, Ruith *et al* [4] show that the obtained flow field is solenoidal within machine accuracy for arbitrary time.

2.1. Existence of breakdown state

Several theories have been proposed to explain the existence of vortex breakdown; however, none has been generally accepted. One school of thought relates breakdown to the existence of standing axisymmetric waves on the vortex core. Standing axisymmetric waves exist only on

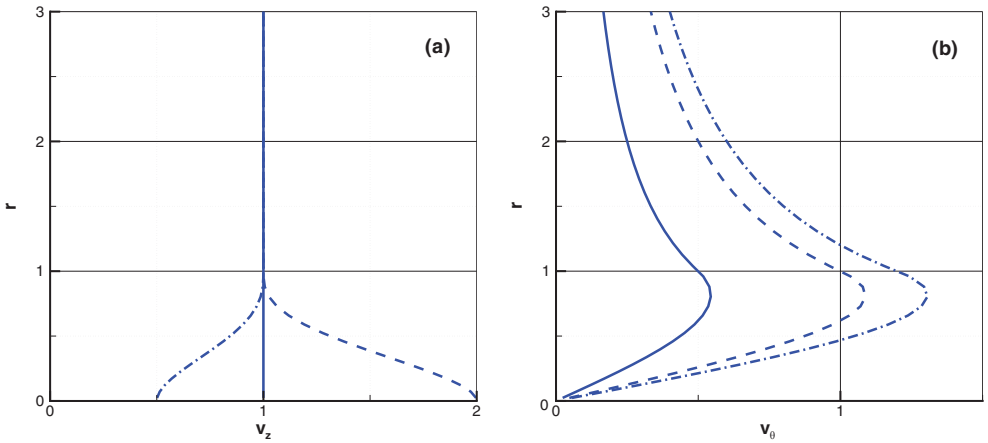

Figure 1. (a) Axial velocity profiles: solid line $\alpha = 1.0$, dashed curve $\alpha = 2.0$, dash–dot curve $\alpha = 0.5$. (b) Azimuthal velocity profiles: solid curve $S = 0.5$, dashed curve $S = 1.0$, dash–dot curve $S = 1.2$. The radial velocity component is zero.

subcritical velocity profiles, while supercritical profiles exclusively support downstream travelling waves. Assuming a steady, axisymmetric and inviscid vortex, Benjamin [2] derives a criticality condition

$$\frac{\mathrm{d}^2\phi_c}{\mathrm{d}r^2} - \frac{1}{r}\frac{\mathrm{d}\phi_c}{\mathrm{d}r} + \left[\frac{1}{r^3\bar{v}_z^2}\frac{\mathrm{d}(r\bar{v}_\theta)^2}{\mathrm{d}r} - \frac{r}{\bar{v}_z}\frac{\mathrm{d}}{\mathrm{d}r}\left(\frac{1}{r}\frac{\mathrm{d}\bar{v}_z}{\mathrm{d}r}\right)\right]\phi_c = 0, \tag{1}$$

starting from the Squire–Long (Bragg–Hawthorne) equation. $\bar{v}_\theta$ and $\bar{v}_z$ represent the azimuthal and axial velocity components of the columnar ($\partial/\partial z = \bar{v}_r = 0$) base flow. Further, Benjamin points out that the homogeneous, linear equation (1) delivers the 'test function' ϕ_c completely except for an arbitrary, constant multiplier. Thus, following Reyna and Menne [5], we choose the boundary conditions to be $\phi_c(r = 0) = 0$ and $\mathrm{d}\phi_c(r = 0)/\mathrm{d}r = 1$, where the latter is arbitrarily chosen to exclude the trivial solution.

Considering Sturm's fundamental comparison theorem, Benjamin and later Mager [2, 6] show that a necessary and sufficient condition for the existence of standing waves of finite length (i.e. for a subcritical state) is that ϕ_c has to vanish at least once in the interval $0 < r < 1$, i.e. between the axis and the characteristic vortex core radius. Applying this analysis to the inflow profile, Grabowski and Berger [1] find no correlation between the occurrence of breakdown and the super- and subcriticality of the inflow profile.

We extend this analysis by applying the criticality condition (equation (1)) to velocity profiles obtained at different axial positions of the axisymmetric, steady state solutions. This is demonstrated in figure 2 for $\alpha = 1.0$ and Reynolds number $Re = 200$ based on the core radius. The left-hand column displays projected streamlines obtained at various swirl numbers S. The right-hand column shows the corresponding criticality character of the velocity profiles as a function of the axial coordinate z by means of a critical radius r_{crit}. The critical radius r_{crit} is equal to the radial position where the test function ϕ_c vanishes. Thus, with the above definition, the flow is subcritical if $r_{crit} < 1$ and supercritical if $r_{crit} > 1$.

The lowest swirl considered ($S = 0.85$) exhibits no internal stagnation point, and the velocity profile remains supercritical everywhere. Increasing the swirl parameter to $S = 0.8944$ an internal stagnation point is observed. This is in agreement with the results of Grabowski and Berger. The flow becomes subcritical upstream of the stagnation point and recovers its supercritical character downstream. Although the columnar assumption is clearly violated

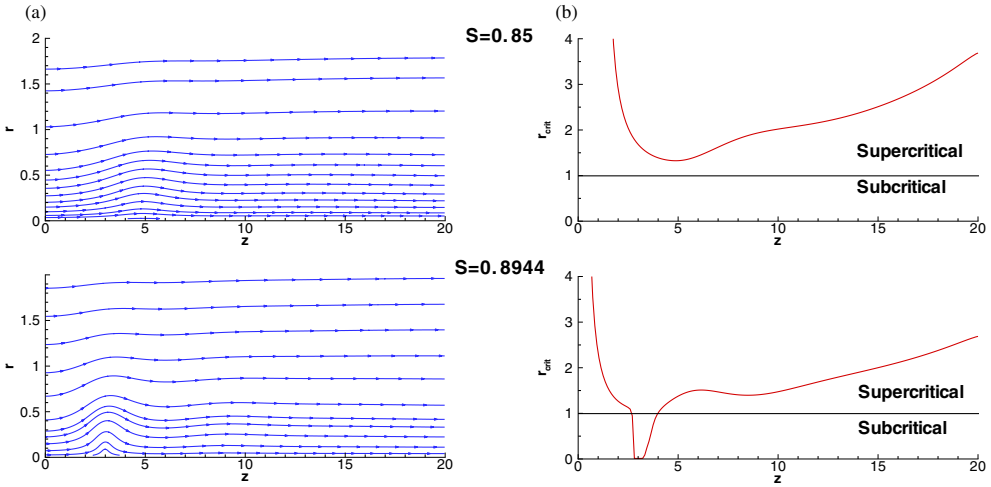

Figure 2. Projected streamlines (left-hand column) together with the criticality of the vortex core (right-hand column) for a swirl number exhibiting no breakdown ($S = 0.85$) and higher swirl $S = 0.8944$ displaying an internal stagnation point. Vortex breakdown is connected to a supercritical/subcritical transition.

around the stagnation point, breakdown is connected to a supercritical/subcritical transition as advocated by Benjamin. Finally we wish to point out that experimental investigations (e.g. [7]) confirm that breakdown represents a transition from supercritical to subcritical flow.

2.2. Transition to different breakdown modes

As pointed out by Escudier *et al* [7], the key to understanding the existence of the wide range of experimentally observed breakdown modes lies in the consideration of the stability towards a discrete spectrum of helical disturbances of the flow field created by the vortex breakdown itself.

For the incipient breakdown state ($S = 0.8944$) discussed above, a stable, axisymmetric state is obtained (not shown here). At larger swirl values ($S = 1.095$), an axisymmetric quasi-steady state develops that displays a pronounced swelling in the wake of the bubble (upper frame in figure 3). The visualization employs streaklines of different colour, consisting of particles which are released close to the axis at the inflow plane. Here an azimuthal instability develops, which ultimately yields a helical breakdown (lower frame in figure 3). By increasing the swirl number to $S = 1.3$, the single helix is replaced by a double-helical breakdown mode (figure 4). The interested reader is referred to the online version of Ruith and Meiburg [8] for an animation of the temporal evolution.

Recently, the formation of a sufficiently large pocket of local absolute instability has been advocated as a possible mechanism causing the transition to the helical breakdown modes. Delbende *et al* [9] and Olendraru *et al* [10, 11] present local absolute/convective instability results for the viscous and inviscid Batchelor vortex, respectively.

Figure 5 displays the regions of stability (S), absolute (AI) and convective (CI) instability. These regions are bounded by solid (viscous) and dashed (inviscid) curves indicating the absolutely unstable wavenumbers m. Assuming that the present velocity profiles at any axial position can be approximated by a Batchelor vortex, we obtain a locus (red curve with filled circles) in the $\alpha - S$ $(a - q)$ parameter space. For $S = 1.095$ (displayed case) two noses reach into the AI region, one corresponding to the bubble, the other to the swelling in the wake of the bubble. The latter starts to reach into the AI region exactly when the transition to a helical

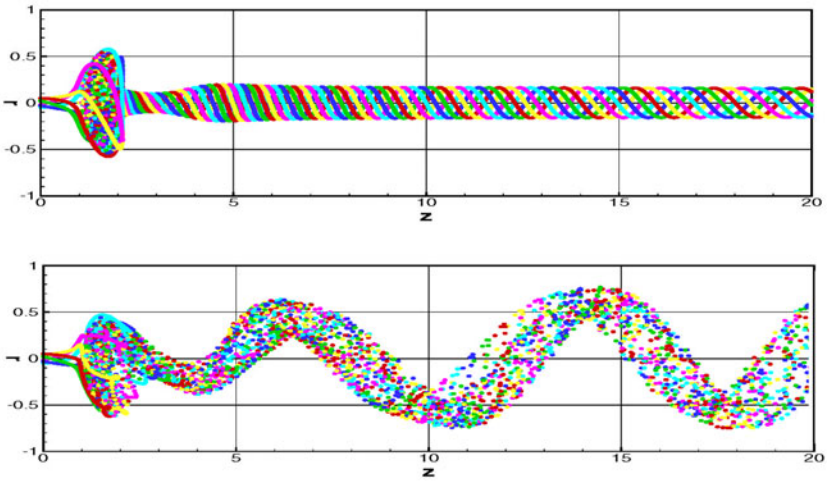

Figure 3. Streaklines at $S = 1.095$. A quasi-steady state (upper frame) at earlier times is superseded by a helical breakdown mode (lower frame).

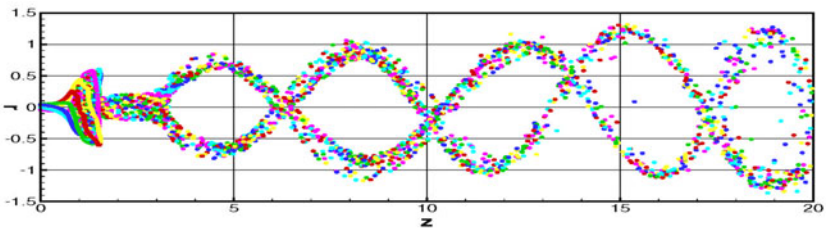

Figure 4. Streaklines at $S = 1.3$ showing a double-helical breakdown structure.

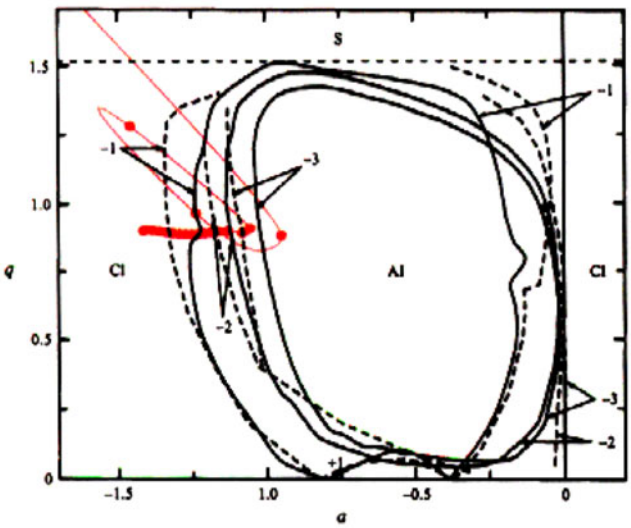

Figure 5. AI/CI transition curves for a Batchelor vortex in the $\alpha - S$ $(a - q)$ parameter space for azimuthal modes $m = \pm 1, -2, -3$. Solid curves: viscous study of Delbende *et al* [9]. Dashed curves: inviscid study of Olendraru *et al* [10, 11]. Red curve with filled circles: present simulation with $S = 1.095$.

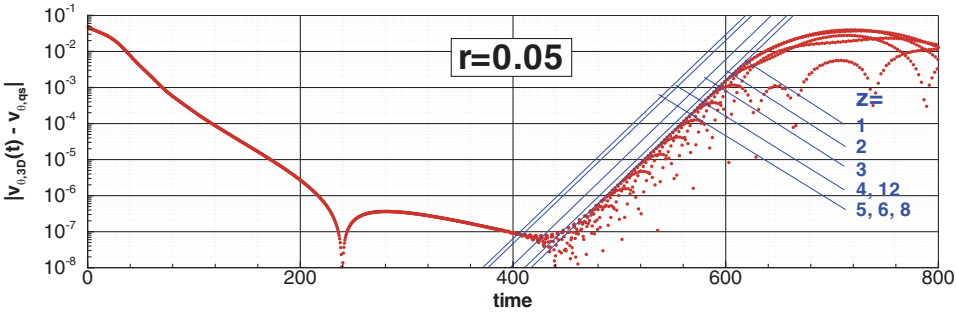

Figure 6. Amplitude of azimuthal velocity v_θ as a function of time at different axial positions for $S = 1.095$

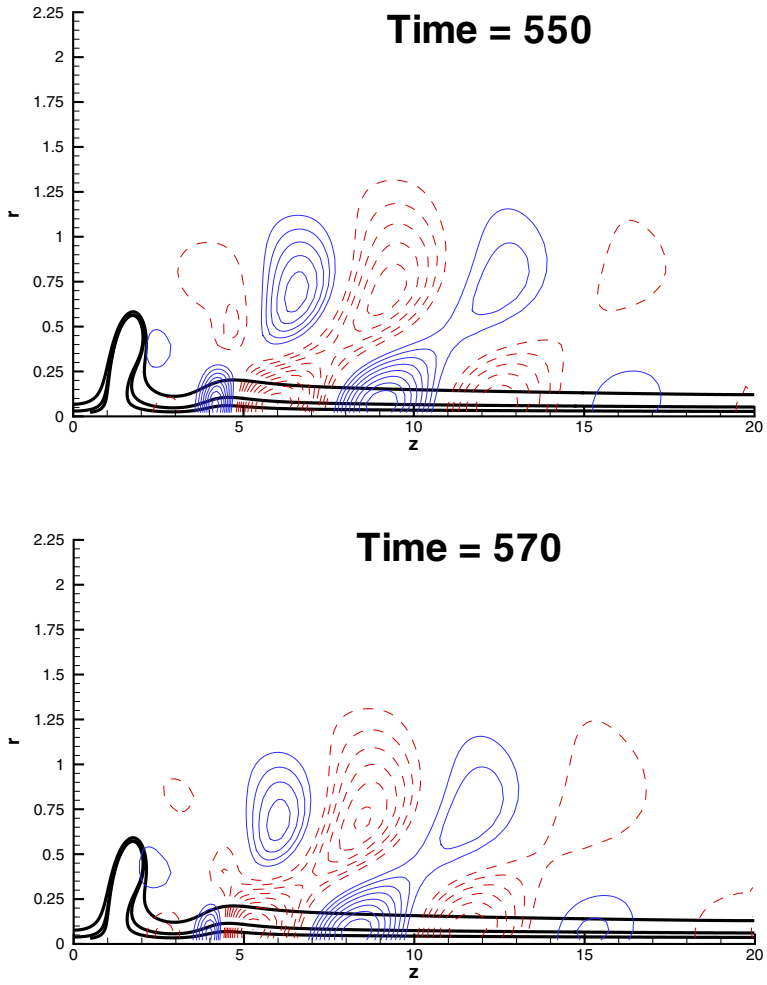

Figure 7. Normalized v_θ-eigenfunctions taken directly from the numerical simulation for $S = 1.095$.

mode is first observed, cf also [12]. Hence, the breakdown mode selection seems to be determined by the existence of local absolute instability, giving rise to a global mode.

This argument is strengthened further by global instability properties obtained directly from the non-linear simulation, cf figure 6. The time dependent, three-dimensional, azimuthal velocity component $v_{\theta,3D}(t)$ settles towards the quasi-steady (qs), axisymmetric bubble breakdown state

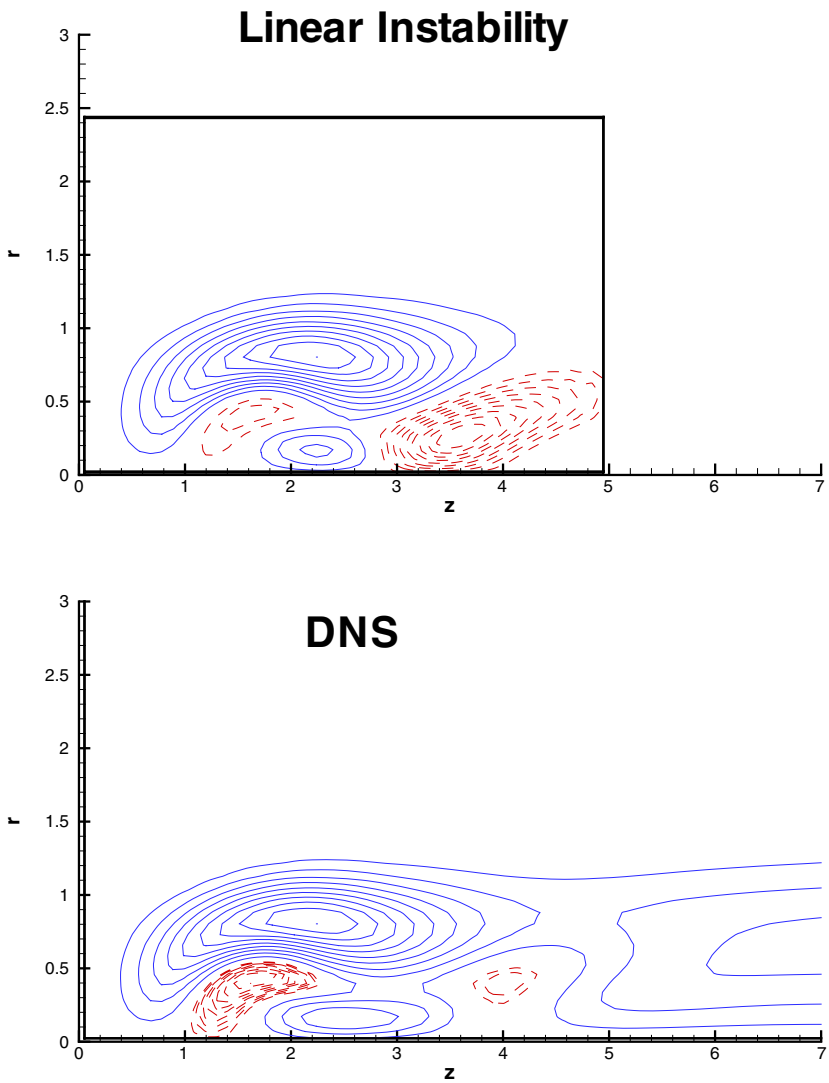

Figure 8. Normalized v_θ-eigenfunction of axisymmetric, linear global stability analysis (top) compared with results obtained directly from the nonlinear simulation (bottom).

$v_{\theta,qs}$. Shortly after time $t = 400$ an exponentially growing global instability takes over, ultimately leading to a helical breakdown mode.

Figure 7 displays the corresponding global v_θ-eigenfunctions at two instances during the exponential growth period. The invariant shape of the eigenfunction reveals a spiralling character which begins around the swelling of the streamtube in the wake of the bubble, confirming local AI/CI results.

Clearly a linear global stability analysis has to deliver corresponding results. We use the word 'global' to stress the fact that the present analysis assumes the base flow and the eigenfunctions to be dependent on the radial and axial coordinate. Thus, in contrast with classical stability analyses, no axial periodicity is assumed. A preliminary result is presented in figure 8 which considers eigenfunctions obtained for an axisymmetric perturbation. The eigenfunctions of the weak damping obtained with the linear global stability analysis (top) and

the nonlinear simulation (bottom) agree very well.

3. Summary and conclusions

We have presented results of linear and nonlinear, axisymmetric and three-dimensional numerical simulations of vortex breakdown. Assuming supercritical inflow profiles it has been shown that the initiation of vortex breakdown corresponds to a transition from supercritical to subcritical as defined by Benjamin [2]. Further, it has been demonstrated that the breakdown mode selection is governed by the formation of a sufficiently large pocket of absolute instability in the wake of the breakdown bubble, giving rise to a global mode.

Acknowledgments

This work was supported by the National Science Foundation. The authors acknowledge several helpful discussions with T Maxworthy and L Redekopp.

References

[1] Grabowski W J and Berger S A 1976 Solutions of the Navier–Stokes equations for vortex breakdown *J. Fluid Mech.* **75** 525–44
[2] Benjamin T B 1962 Theory of the vortex breakdown phenomenon *J. Fluid Mech.* **14** 593–629
[3] Maxworthy T 2001 Private communication
[4] Ruith M R, Chen P and Meiburg E 2002 Optimal boundary conditions for direct numerical simulations of three-dimensional vortex breakdown phenomena in semi-infinite domains *Comput. Fluids* submitted
[5] Reyna L G and Menne S 1988 Numerical prediction of flow in slender vortices *Comput. Fluids* **16** 239–56
[6] Mager A 1972 Dissipation and breakdown of a wing-tip vortex *J. Fluid Mech.* **55** 609–28
[7] Escudier M P, Bornstein J and Maxworthy T 1982 The dynamics of confined vortices *Proc. R. Soc.* A **382** 335–60
[8] Ruith M R and Meiburg E 2002 Breakdown modes of swirling jets with coflow *Phys. Fluids* **14** S11
[9] Delbende I, Chomaz J-M and Huerre P 1998 Absolute/convective instabilities in the Batchelor vortex: a numerical study of the linear impulse response *J. Fluid Mech.* **355** 229–54
[10] Olendraru C, Sellier A, Rossi M and Huerre P 1996 Absolute/convective instability of the Batchelor vortex *C. R. Acad. Sci. Paris* II **323** 153–9
[11] Olendraru C, Sellier A, Rossi M and Huerre P 1999 Inviscid instability of the Batchelor vortex: absolute–convective transition and spatial branches *Phys. Fluids* **11** 1805–20
[12] Chen P 2000 Numerical simulations of swirling flows *PhD Thesis* Department of Aerospace and Mechanical Engineering, USC